J. Quant. Spectrosc. Radiat. Transfer Vol. 21, pp. 11–18

0022-4073/79/0101-0011/$02.00/0

SATURATION OF SODIUM FLUORESCENCE IN A FLAME IRRADIATED WITH A PULSED TUNABLE DYE LASER

R. A. VAN CALCAR, M. J. M. VAN DE VEN, B. K. VAN UITERT, K. J. BIEWENGA, TJ. HOLLANDER, and C. TH. J. ALKEMADE
Fysisch Laboratorium, Universiteit, Utrecht, The Netherlands

(*Received* 1 *June* 1978)

Abstract—Theoretical and experimental saturation curves and associated saturation parameters for the Na-*D* doublet in an H_2–O_2–Ar flame at 1 atm ($T = 1700$ K) are compared. These parameters are found to agree within the experimental error of 25%. An explanation based on the spatial and temporal distribution of the laser intensity is given for the deviating saturation curves reported by various authors. The shape of the fluorescence pulse is shown to depend on the O_2 concentration in the flame. A lower limit for the rate constant of the doublet mixing transition is estimated from the ratio of the saturated fluorescence intensities of the Na-*D* components and found to be 3×10^8 s^{-1}. Conclusions are drawn which restrict the use of saturated atomic fluorescence intensities as a measure for the total atomic number density in the flame.

INTRODUCTION

DURING the last few years, an increasing number of articles has been published[1–4] describing measurements of saturated sodium fluorescence in flames. These papers report on the dependence of the relative fluorescence intensity on the laser irradiance (saturation curve) and comment on the determination of the saturation parameter. In all of these papers, deviations from the theoretical curve and/or the theoretical saturation parameter were found to be fairly large. An explanation for these deviations is given based on the following considerations: In general the laser pulse decays gradually and the duration of the saturated fluorescence pulse depends on the peak value of the laser pulse. Therefore, the integrated fluorescence intensity, although saturated, still depends on the laser intensity. The non-uniform spatial distribution of the laser beam has a similar effect on the saturation curve, as was pointed out by DAILY.[5] The depletion of neutral Na atoms by (chemical) reactions complicates measurements of the saturation curve and the saturation parameter in yet another way. Measurements have to be carried out under conditions which ensure that these disturbing effects are eliminated. A discussion of these considerations, together with preliminary results, has been presented by ALKEMADE.[6]

THEORETICAL CONSIDERATIONS

In order to derive a theoretical value for the saturation parameter for the Na-*D* lines, we use a three-level model for the sodium atom, neglecting transitions from the Na-*D* levels to higher levels and to the ionization continuum. Because the rise time and the duration of the laser pulse are long compared with characteristic atomic lifetimes (inverse collisional and radiation rate constants), the conventional rate equations are used to describe the system in the stationary state.[7] The spectral volume density of the laser radiation field is assumed to be constant over the atomic line width since the laser bandwidth is larger than the absorption line width in the flame (but small enough to excite only one of the Na-*D* lines). In solving the rate equations in the stationary case, we neglect the thermal excitation from the ground state; this procedure is justified in the light of our experiments. We denote the transition rate constant from level i to level j by a_{ij}, the ground level by index 1 and the laser-excited doublet component by index 3. The various transition rate constants a_{ij} are given by $a_{13} = B_{13}\rho_\nu$, $a_{31} = B_{31}\rho_\nu + A_{31} + k_{31}$, $a_{12} = 0$, $a_{21} = A_{21} + k_{21}$, $a_{32} = k_{32}$ and $a_{23} = k_{23}$. Here B_{31} = the Einstein coefficient for stimulated emission (cm^3 J^{-1} s^{-2}); B_{13} = the Einstein coefficient for absorption (cm^3 J^{-1} s^{-2}); A_{31} and A_{21} = the Einstein coefficients for spontaneous emission (s^{-1}); k_{31} and k_{21} = the monomolecular quenching rate constants (s^{-1}); k_{32} and k_{23} = the monomolecular mixing rate constants (s^{-1}); ρ_ν = the

spectral volume density of the radiation field in the flame ($J \cdot cm^{-3} Hz^{-1}$) which is tuned to the 1–3 transition.

Using the relation $B_{13} = (g_3/g_1)B_{31}$ (where g_1 and g_3 are the statistical weights), we find the following solutions for the relative number densities n_i of the atoms in the three levels:

$$\frac{n_3}{n_t} = \frac{A_{21} + k_{21} + k_{23}}{D} \times \frac{\rho_\nu}{\rho_\nu + \rho_\nu^s} \tag{1}$$

$$\frac{n_2}{n_t} = \frac{k_{32}}{D} \times \frac{\rho_\nu}{\rho_\nu + \rho_\nu^s} \tag{2}$$

$$\frac{n_1}{n_t} = \frac{(g_1/g_3)(A_{21} + k_{21} + k_{23})}{D} \times \frac{\rho_\nu}{\rho_\nu + \rho_\nu^s} + \frac{\rho_\nu^s}{\rho_\nu + \rho_\nu^s} \tag{3}$$

with $D \equiv (1 + g_1/g_3)(A_{21} + k_{21} + k_{23}) + k_{32}$. The quantity $n_t \equiv n_1 + n_2 + n_3$ is the total atomic number density (cm^{-3}). The quantity ρ_ν^s is the saturation parameter, which is defined as the value of the spectral volume density at which the relative population density of the laser-excited level is half its limiting value for $\rho_\nu \to \infty$. Another definition for the saturation parameter, equivalent to the one just given, is the following: ρ_ν^s represents the value of the spectral volume density at which the population density of the laser-excited level is one half of its value on the extrapolated initial asymptote. Accordingly,

$$\rho_\nu^s = (g_1/g_3) \frac{(A_{31} + k_{31})(A_{21} + k_{21}) + (A_{31} + k_{31})k_{23} + (A_{21} + k_{21})k_{32}}{B_{31}D}. \tag{4}$$

For the population ratio of the two upper levels we find from Eq. (1) and Eq. (2)

$$\frac{n_3}{n_2} = \frac{k_{23}}{k_{32}} + \frac{A_{21} + k_{21}}{k_{32}}. \tag{5}$$

These equations are in agreement with relations given in Ref. (5). Making use of the small energy difference between the two doublet levels compared to the large value of kT at the flame temperature (1700 K), we write $k_{23}/k_{32} = g_3/g_2$. We simplify Eqs. (1)–(5) by substituting this expression for k_{23}/k_{32} and making the approximations $A_{31} \approx A_{21} \equiv A$, $k_{31} \approx k_{21} \equiv k$, $B_{31} \equiv B$. We also use the relations $B = (c^3/8\pi h\nu^3)A$ and $A/(A + k) \equiv Y$, where c = speed of light *in vacuo* ($cm \cdot s^{-1}$), h = Planck's constant ($J \cdot s$), ν = mean frequency of the two D lines (Hz), and Y = the efficiency of fluorescence. Within an error of 2% the following equations hold:

$$\frac{n_3}{n_t} = \frac{A/Y + (g_3/g_2)k_{32}}{D'} \times \frac{\rho_\nu}{\rho_\nu + \rho_\nu^s} \tag{6}$$

$$\frac{n_2}{n_t} = \frac{k_{32}}{D'} \times \frac{\rho_\nu}{\rho_\nu + \rho_\nu^s} \tag{7}$$

$$\frac{n_1}{n_t} = \frac{(g_1/g_3)(A/Y + (g_3/g_2)k_{32})}{D'} \times \frac{\rho_\nu}{\rho_\nu + \rho_\nu^s} + \frac{\rho_\nu^s}{\rho_\nu + \rho_\nu^s} \tag{8}$$

with $D' \equiv [1 + (g_1/g_3)]A/Y + [1 + (g_1/g_2) + (g_3/g_2)]k_{32}$ and

$$\rho_\nu^s = (g_1/g_3) \frac{8\pi h\nu^3}{c^3} \times \frac{A/Y + (1 + g_3/g_2)k_{32}}{YD'} \tag{9}$$

$$\frac{n_3}{n_2} = g_3/g_2 + \frac{A}{Yk_{32}} = (g_3/g_2)\left(1 + \frac{A + k}{(g_3/g_2)k_{32}}\right). \tag{10}$$

The population ratio of the two doublet levels therefore depends on the ratio of the sum of the

spontaneous emission and quenching rate constants to the doublet mixing rate constant. From Eq. (10), it is seen that an experimental value for k_{32} can be obtained by measuring the ratio of the fluorescence intensities of the two D lines and Y. If $(A/Yk_{32}) \ll 1$, Eq. (9) can be approximated by

$$\rho_\nu^s = (g_1/g_3)\frac{8\pi h\nu^3}{c^3} \times \frac{g_2+g_3}{g_1+g_2+g_3}(1/Y). \tag{11}$$

Substituting the appropriate values of the statistical weights into Eq. (11), we obtain within 3% accuracy, for $(A/Yk_{32}) \ll 1/3$,

$$\rho_\nu^s = 3\frac{\pi h\nu^3}{c^3}(1/Y), \tag{12}$$

if the upper doublet level is directly excited by the laser beam. If the lower doublet level is directly excited, we obtain within 6% accuracy, for $(A/Yk_{23}) \ll 1/3$,

$$\rho_\nu^s = 6\frac{\pi h\nu^3}{c^3}(1/Y). \tag{13}$$

The saturation parameter and the population ratio of the doublet levels therefore depend on which of the doublet levels is directly excited by the laser irradiation.

EXPERIMENTAL SETUP AND PROCEDURE

In our experiments, we used a flashlamp-pumped dye laser (Zeiss FL 3A) with an effective pulse duration of 460 ± 20 ns. Since the typical time constants of the atomic system are of the order of ions, the assumption that the stationary case applies is justified. The spectral half-intensity width (FWHM) of the laser is 150 ± 20 mÅ (or $(1.3 \pm 0.2) \times 10^{10}$ Hz). The FWHM of the Na-D absorption line profiles is 80 ± 10 mÅ [according to our measurements with a Fabry–Pérot interferometer and measurements by WIJCHERS[8]]. Therefore, the laser can be considered to be a quasi-continuous spectral radiation source as far as the excitation of the atomic transition is concerned; on the other hand, only one of the doublet components will be excited.

Photographic measurements of the laser beam have indicated that the spatial distribution across the laser beam is not Gaussian [as was assumed in the theoretical calculations of DAILY[5]]. The photographs revealed a central beam with a divergence of about 5 mrad, surrounded by a second beam with a greater divergence of about 10 mrad and with a ring structure in the outer parts. At the flame, the over-all cross section of the beam appeared to be slightly oval, with the long axis being about 1 cm in the horizontal direction (the direction of observation of fluorescence).

Attenuation of the laser beam irradiance was achieved with calibrated neutral density filters so that the temporal, spatial and spectral properties of the laser pulse did not change upon attenuation. The filters were placed at an angle of 65° with respect to the laser beam to avoid

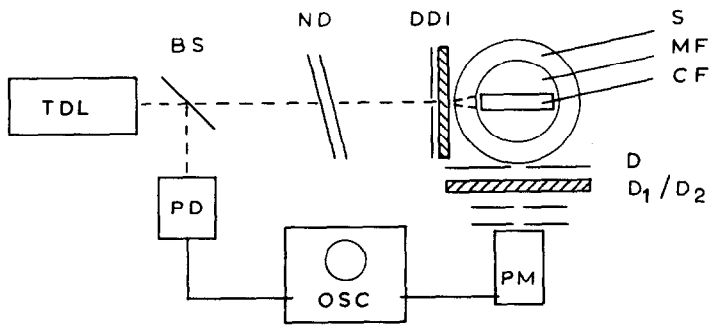

Fig. 1. Schematic diagram of the experimental arrangement; *TDL*—pulsed tunable dye laser, *BS*—beam splitter, *ND*—neutral density filter, *D*—diaphragms, *Di*—diffuser, *S*—Ar sheath, *MF*—mantle flame, *CF*—central flame, D_1/D_2—spectral filter, *PD*—photodiode, *OSC*—oscilloscope and *PM*—photomultiplier tube.

disturbing reflections. The change in the transmission factor of the filters, brought about by turning them 25°, causes an error which is small compared to the other experimental errors.

To detect the time-resolved fluorescence pulses, a fast photo-multiplier tube was used in combination with an oscilloscope. By means of a spectral filter that transmits either one or the other component of the Na-*D* doublet, it was possible to measure separately the saturation curves of the doublet components. By measuring the saturation curve of the component that is not directly excited by the laser, one avoids possible interference from the laser straylight.

All of our experiments were carried out in a laminar, premixed H_2–O_2–Ar flame ($T = 1700 \pm 50$ K) with a nearly stoichiometric H_2–O_2 composition. It was produced on a Mékèr burner at 1 atm and shielded from the surrounding air by an Ar-sheath.[9]

The measurement of fluorescence intensities in relation to laser irradiance appeared to cause various problems.

In the first place, the temporal behaviour of the laser pulse may give rise to a distorted saturation curve and therefore to an anomalous value for the saturation parameter if time-integrated fluorescence measurements are carried out. If the laser pulse does not instantly drop to zero but decays gradually, the duration of saturated fluorescence (i.e. $\rho_\nu > \rho_\nu^s$) will increase with the laser peak-intensity. This result is illustrated by the calculated pulse shapes in Fig. 2. Consequently, the time-integrated fluorescence intensity will continue to increase with the laser peak-intensity. Figure 3 shows this effect on the saturation curve, calculated under the conditions assumed in Fig. 2. By measuring time resolved fluorescence intensities, one can obtain the true saturation curve and avoid this artefact. This fact is experimentally demonstrated in Fig. 4.

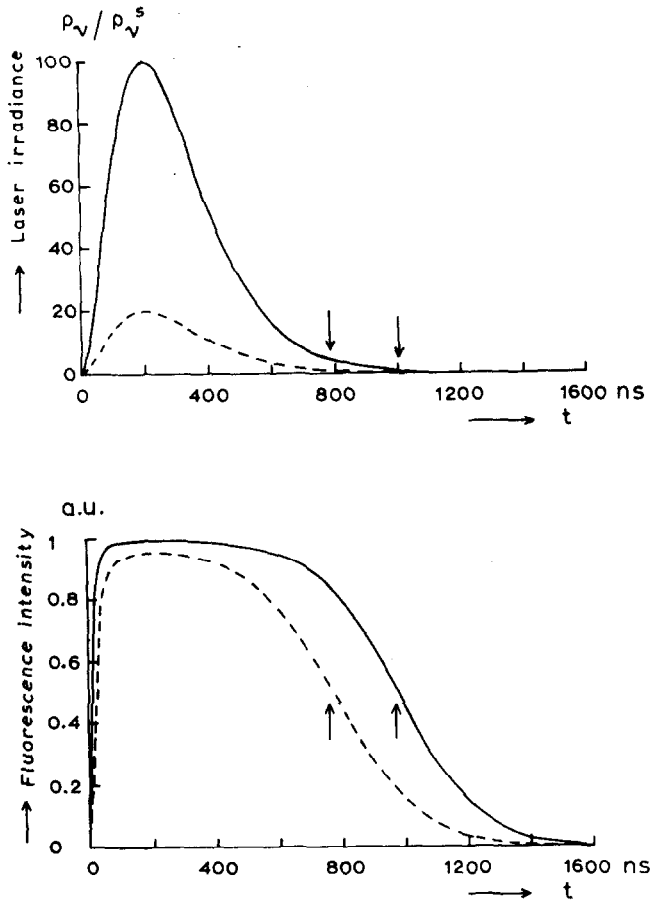

Fig. 2. Illustration of the effect of time integration of the fluorescence pulse. The laser pulse is assumed to decay exponentially. The calculated integrated fluorescence pulse under saturation conditions continues to increase with the laser (peak) intensity because the duration of saturation increases with it. The arrows indicate the points where $\rho_\nu/\rho_\nu^s = 1$.

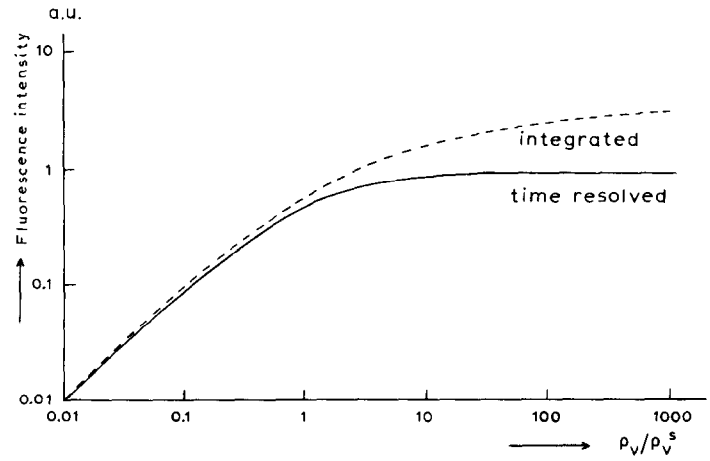

Fig. 3. Calculation of the effect of time integration of the fluorescence pulse on the shape of the saturation curve. The laser pulse is assumed to decay exponentially as in Fig. 2.

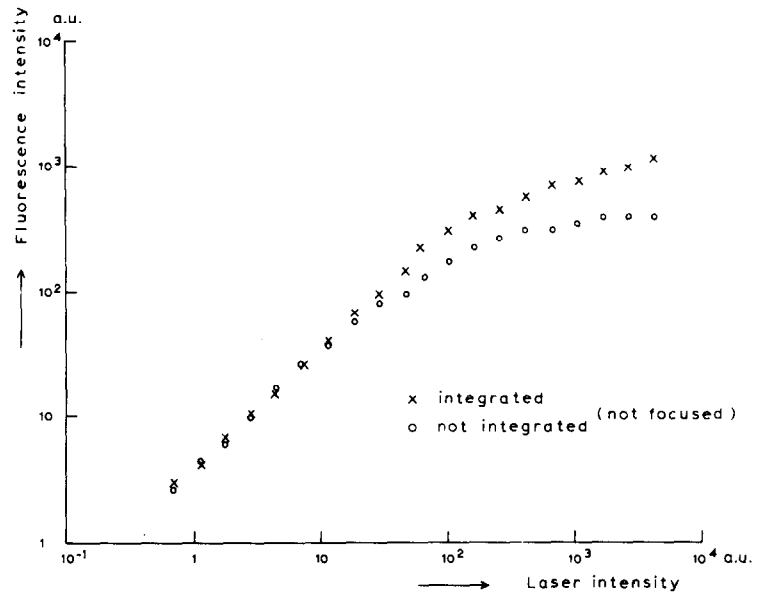

Fig. 4. Experimental demonstration of the effect of time integration of the fluorescence pulse on the saturation curve.

In the second place, the spatial distribution of the laser irradiance in the flame can affect the shape of the saturation curve and so result in an anomalous saturation parameter. As was pointed out by RODRIGO and MEASURES[10] and calculated by DAILY[5] for some special cases, a plateau in the saturation curve will not be found unless the spatial distribution of the laser irradiance in the observed part of the flame is uniform. Especially when the laser beam is focused to a spot that is small compared with the flame thickness, large deviations may occur. Figure 5 shows an experimental illustration of this effect.

In order to avoid the effects of spatial inhomogeneities mentioned above, we did not use focusing lenses. A flame geometry with a rectangular cross section (3×0.8 cm) was constructed (see Fig. 1) and low Na concentrations were used to avoid self-absorption effects and to improve the uniformity of the irradiance along the beam axis. A diaphragm with a diameter of 0.80 ± 0.02 cm was placed in the laser beam just in front of the flame in order to enhance the uniformity of the irradiance in the direction of the detection channel (perpendicular to the beam axis). By means of two diaphragms in the detection channel, the uniformity of the laser irradiance in the observed part of the flame was further improved.

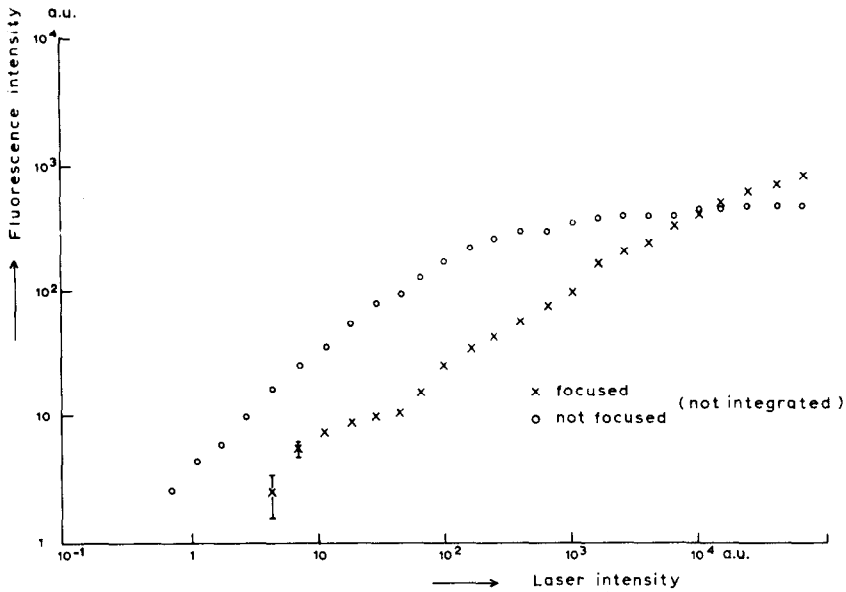

Fig. 5. Experimental demonstration of the effect of spatial inhomogeneity of the laser irradiance on the shape of the saturation curve. The effect is caused by focusing the laser beam in the flame.

Per pulse calibration of the radiant energy of the laser beam was performed with a power meter (Molectron, type J-03). In order to convert this radiant energy to spectral volume density in the flame, the beam must be made homogeneous over its entire cross section and not only over that part of its cross section registered by the detection apparatus. This design was achieved by attaching a diffuser to the diaphragm in the laser beam. This device diffuses the beam only slightly. A disadvantage of using the diffuser is the considerable loss of spectral volume density at the flame; however, the remaining density is still sufficient to exceed ρ_ν^s by a factor of 10. The spectral volume density (in $J \cdot cm^{-3} Hz^{-1}$) is calculated from

$$\rho_\nu = Q/\Delta t S c \delta\nu. \tag{14}$$

Here Q = the radiant energy per pulse (J), Δt = the effective duration of the pulse (s), S = the beam cross section (cm^2), c = the speed of light *in vacuo* ($cm \cdot s^{-1}$), and $\delta\nu$ = the spectral half-intensity width (Hz) of the laser light. Photographic measurements show a beam cross-section $S = 0.5 \pm 0.1\ cm^2$ at the flame.

RESULTS

A lower limit for the doublet mixing-rate constant was estimated from measurements of the ratio of the fluorescence intensities for the two D lines. The ratio D_2/D_1 is 1.69 ± 0.15 if D_1 is excited and 2.20 ± 0.10 if D_2 is excited. From these two values, we calculate from Eq. (10) a lower limit for the mixing rate constant $k_{32} = 3 \times 10^8\ s^{-1}$, in which the subscript 3 refers to the upper doublet level and the 2 to the lower level. The approximate expression in Eq. (11) is therefore applicable to our experimental conditions. In a flame with the same composition and the same temperature and pressure, a value $k = (3.7 \pm 0.6) \times 10^7\ s^{-1}$ for the quenching rate constant has been reported by LUNSE and ELSENAAR.[9] Now we calculate $Y = 0.63 \pm 0.04$ using $A = (6.2 \pm 0.1) \times 10^7\ s^{-1}$ as given by MASHINSKII.[11] Substitution in Eq. (11) gives $\rho_\nu^s = (4.8 \pm 0.3) \times 10^{-20}\ J \cdot cm^{-3} Hz^{-1}$ if the upper doublet level is excited and $\rho_\nu^s = (9.7 \pm 0.6) \times 10^{-20}\ J \cdot cm^{-3} Hz^{-1}$ if the lower doublet level is excited.

Measurements of saturation curves were carried out in two stages. First, a saturation curve along an absolute ρ_ν-axis was measured with the diffuser in the laser beam. From this curve, the saturation parameter was derived in absolute measure by fitting the theoretical saturation curve, Eq. (7), to the experimental points. Secondly, a saturation curve along a relative ρ_ν-axis was measured without the diffuser in the beam so that higher laser irradiances could be reached. From this curve, we derived a relative saturation parameter and assumed it to have the same

value as in the first measurement. In this way, the two experimental curves were linked together. Figure 6 gives a saturation curve obtained by this procedure.

The value of the saturation parameter ρ_ν^s is $(5.6 \pm 1.4) \times 10^{-20}\,\mathrm{J \cdot cm^{-3}\,Hz^{-1}}$ (corresponding to an irradiance of $22 \pm 4\,\mathrm{W \cdot cm^{-2}}$) if the laser couples the ground level and the upper doublet level while its value is $(9.0 \pm 2.3) \times 10^{-20}\,\mathrm{J \cdot cm^{-3}\,Hz^{-1}}$ (corresponding to an irradiance of $35 \pm 10\,\mathrm{W \cdot cm^{-2}}$) if the laser couples the ground level and the lower doublet level. Both experimental values are in agreement with the calculated values within the experimental error of 25%; the errors are mainly due to inaccuracies in the calibration of the laser irradiance.

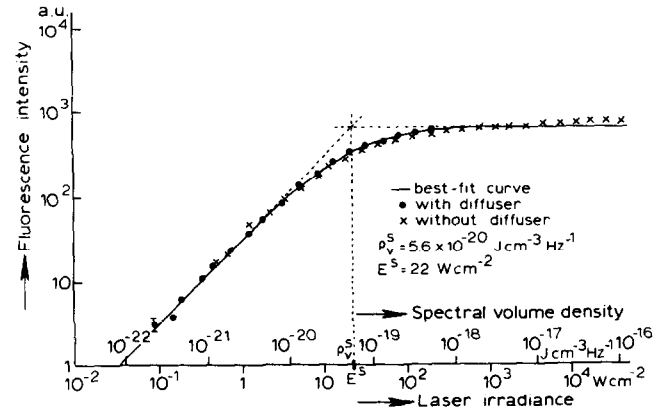

Fig. 6. An experimental saturation curve of the Na-D_1 line with the laser tuned at the D_2 line. The drawn curve represents the best fit of the theoretical curve [see Eq. (7)] to the experimental points obtained with a diffuser in the beam.

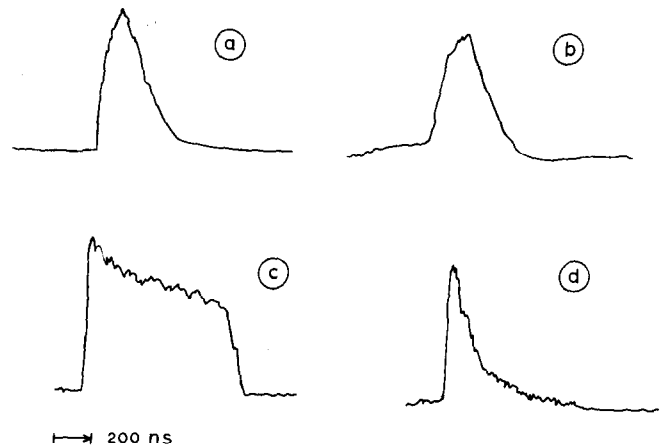

Fig. 7. Oscilloscope traces of experimental pulse shapes. (a) laser pulse; (b) fluorescence pulse, not saturated; (c) saturated fluorescence pulse in an O_2-lean flame. The saturated fluorescence pulse lasts longer than the FWHM duration of the laser pulse (compare Fig. 2). (d) saturated fluorescence pulse in an O_2-rich flame.

When the O_2/H_2 gas flow ratio was varied, the fluorescence pulse shape appeared to be strongly dependent on the free O_2 concentration in the flame at high laser irradiance (see Fig. 7). The peak in the fluorescence pulse is followed by a gradual decay, the extent of which depends on the O_2 concentration. Addition of another molecular species such as N_2 caused no such effects.

The ionization energy for the excited Na atoms is 2.1 eV lower than that of Na atoms in the ground state. Consequently, the activation energy for an ionizing collision of excited Na atoms is decreased by the same amount. The electron affinity of O_2 has a positive value [about 0.5 eV[12]], whereas the electron affinity of N_2 has a negative value (about -2.0 eV). The positive value of the electron affinity of O_2 decreases the activation energy for an ionizing collision further. A calculation of the degree of ionization, α, in the steady state for Saha equilibrium between Na atoms and Na^+ ions in our flame shows a value of 4×10^{-4} for Na atoms in the

ground state. Under saturation conditions, Saha equilibrium also exists between Na^+ ions and excited Na atoms. In this case, we calculate $\alpha = 0.5$. In 0_2-rich flames, the activation energy of the ionization reaction is further reduced and we calculate $\alpha = 0.95$.

The positive electron affinity of O_2 also affects the value of the ionization rate constant.[13] Under saturation conditions, the ionization rate constant is some 100 times larger for O_2 as the collision partner than for N_2. In absolute value, its reciprocal becomes of the order of the pulse duration if O_2 is the collision partner.

All of our measurements on saturation curves were carried out in a flame with a low O_2 concentration in order to avoid this complication. As a result of this precaution, the plateau and peak values of the fluorescence pulse, as in Fig. 7(c), give the same value for the saturation parameter.

DISCUSSION

We have verified the theoretically predicted shape of the saturation curve and the value of the saturation parameter. Agreement between theory and experiment was achieved within 25% by using a diffuser in the laser beam and by reducing the distorting effects of spatial and temporal non-uniformity of the laser beam irradiance upon the saturation curve. A residual effect is still detected at very high laser irradiances. The error in ρ_ν^s is mainly due to uncertainty in the spatial intensity distribution of the laser beam.

The systematic deviations from the value 2 of the D_2/D_1 fluorescence ratio found by DAILY[14] in a methane-air flame at 1 atm when the laser was tuned to the D_1 and the D_2 line, respectively, can be readily understood when Eq. (10) is applied. In a methane-air flame, a high value for the overall quenching rate constant can be expected due to the presence of CO, CO_2 and N_2 in the flame. According to Eq. (10), a high value for the overall quenching rate constant causes deviations from 2 for the D_2/D_1 fluorescence ratio, although the mixing rate constant may be large.

Depletion of neutral Na atoms by collisional ionization of excited Na atoms by O_2 molecules can explain why the fluorescence pulse shape under saturation conditions depends on the O_2 concentration in the flame. This explanation agrees with electric probe measurements by VAN DIJK,[15] which show an increase in the ratio of the ionization signal to the fluorescence signal with increasing O_2 concentration in an identical flame.

The use of saturated atomic fluorescence spectroscopy (SAFS) to determine the total number density of Na atoms in a flame[14] is restricted by the complications mentioned above.

Acknowledgements—The authors wish to thank the ZWO (Netherlands Organisation for pure Scientific Research) for providing financial support for part of this work and MISS S. M. MCNAB for taking care of some linguistic elements.

REFERENCES

1. J. KUHL, S. NEUMANN and M. KRIESE, *Z. Naturforsch.* **A28**, 273 (1973).
2. B. L. SHARP and A. GOLDWASSER, *Spectrochim. Acta* **31B**, 431 (1976).
3. D. RIJAS DE OLIVARES, Ph.D. Thesis, Indiana University, U.S.A. (1976).
4. B. SMITH, J. D. WINEFORDNER and N. OMENETTO, *J. Appl. Phys.* **48**, 2676 (1977).
5. J. W. DAILY, *Appl. Opt.* **17**, 225 (1978).
6. C. TH. J. ALKEMADE, *7th Int. Conf. on Atomic Spectrosc.* Prague (1977), *Invited Lectures, Sbornik VSCHT*, 93 (1977).
7. J. W. DAILY, *Appl. Opt.* **16**, 2322 (1977).
8. T. WIJCHERS, University of Utrecht, The Netherlands, personal communication.
9. P. L. LIJNSE and R. J. ELSENAAR, *JQSRT* **12**, 1115 (1972).
10. A. B. RODRIGO and R. M. MEASURES, *IEEE. J. Quantum Electron.* **QE-9**, 972 (1973).
11. A. L. MASHINKII, *Opt. Spectrosc.* **28**, 1 (1970).
12. A. P. M. BAEDE, *Advances in Chemistry Physics* (1975), (Edited by K. P. LAWLEY) Vol. 30, p. 463. Wiley, New York.
13. TI. HOLLANDER, P. J. KALFF and C. TH. J. ALKEMADE, *J. Chem. Phys.* **39**, 2558 (1963).
14. J. W. DAILY, University of California, Berkeley, U.S.A. personal communication.
15. C. A. VAN DIJK, University of Utrecht, The Netherlands, personal communication.